Jurnal Teknologi

Full Paper

NUMERICAL ANALYSIS OF MODIFIED ANGLE OF ENTRANCE AND DUCKTAIL ADDITION OF THE 1,500 GT RO-RO FERRY HULL VALIDATED WITH SHIP MODEL RESISTANCE TEST

Cahyadi Sugeng Jati Mintarso[a,b]*, Semin[a], Erwandi[b], Dian Purnamasari[b]

[a]Department of Marine Engineering, Faculty of Marine Technology, Institut Teknologi Sepuluh Nopember (ITS), Keputih, Sukolilo, Surabaya, 60111, Indonesia
[b]The National Research and Innovation Agency, Jl. Hidrodinamika, Keputih, Kec. Sukolilo, Surabaya, Indonesia, 60112, Indonesia

Article history
Received
26 November 2022
Received in revised form
12 June 2023
Accepted
19 June 2023
Published Online
21 August 2023

*Corresponding author
6019211007@mhs.its.ac.id

Graphical abstract

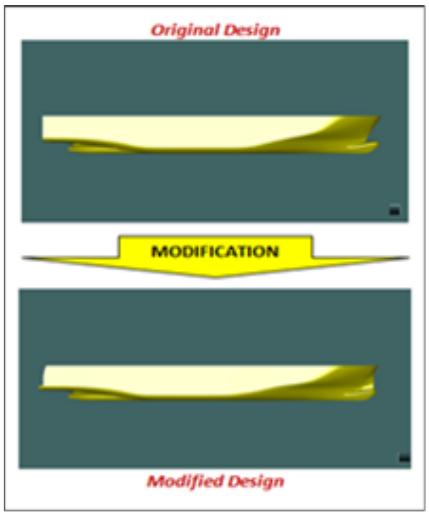

Abstract

The main problem of ferry ships is maintaining the speed due to ship resistance. There are many efforts to reduce the resistance by modifications of them. This study aims to reduce resistance due to modification of the hull form on the bow Angle of Entrance (AoE) and ducktail addition at the transom stern. The object of the research is a 1,500 GT ro-ro ferry. The AoE minimizes wave resistance and improves flow patterns, while the ducktail reduces the negative effects of the circulation zone on the wetted transom so that waves and wake are reduced. Computational Fluid Dynamics (CFD) was used to analyze these modifications. The final results of the numerical simulation are then verified by the ship model resistance test in the towing tank. Tests were conducted in calm water conditions at a draft of 3.30 meters with a speed variation of 10 - 18 knots. The results show that with the combination of AoE and Ducktail, at ship speeds of 13 to 18 knots, the reduction in resistance from CFD ranges from 13.13% - 16.69% while the experimental results range from 16.00% - 16.54%. While separately the AoE modification is between 8.89% – 12.19% and ducktail is 3.12% -3,62%.

Keywords: Angle of entrance, computational fluid dynamics (CFD), ducktail, towing tank, resistance test

1.0 INTRODUCTION

Indonesia, as a maritime and archipelagic country, needs ferries for island connectivity and the development of the remote areas. They can connect and transport goods and services between islands [1]. As sea transportation mode, ferries prioritize safety, speed, and efficiency based on hull, engine, propulsion, and route. In addition to functioning as connectivity, it is also a relatively low-cost mode of sea transportation with a large passenger/goods carrying capacity. Ferries are also a key factor that plays an important and strategic role and is expected to support national economic growth.

On the other hand, energy-efficient measures like EEDI (Energy Efficiency Design) and alternative fuels can overcome speed and emissions issues. Reducing

exhaust emissions from ship operations to protect the maritime environment can be done by implementing energy efficiency (amount of fuel consumption). The EEDI Index [2] aspect required by the International Maritime Organization (IMO) in terms of reducing the value of ship resistance is still considered very low [3]. Some of the anticipations are the use of alternative fuels, energy-saving machines, designing efficient new ships, or modifying existing ships [4]. Decreased speed due to large resistance, is often a major problem on ships, especially ferries.

Ro-ro ferries are a mode of sea transportation whose operations focus on speed, safety, and energy efficiency. This demand is due to the fact that operational optimization is highly dependent on the shape of the hull, engine, propulsion system, and shipping route [5].

Various efforts have been made to reduce the total resistance of the ship. Some of them are modifying the hull form [6], installing the undership fin to improve the direction of the fluid flow under the hull to the propeller [7], providing the bulbous bow to decrease wave interference which contribute to reduce ship wave resistance [8, 9], attaching stepped hull to reduce the wetted surface area [10, 11], sharpening the bow AoE [12, 13, 14, 15] and the addition of the ducktail at the transom stern [16, 17, 18] to reduce viscous and wave resistance.

Modifying the AoE and adding a ducktail is common practice to optimize the ferry's resistance. The AoE at the bow of the ship serves to improve the performance of the ship, which is closely related to resistance due to waves. The shape of the bow hull with a sharper AoE allows waves to follow the bow more smoothly. Reducing AoE serves to minimize wave resistance [12, 13, 14, 15, 19] and improve flow patterns [20]. The movement of the ship always causes waves. The AoE of the ship's bow waterline affects the size of the waves that occur. Because of that, the ship's bow is made in the best possible shape to avoid the big waves that occur. Therefore the modification of AoE is required to reduce the ferry's resistance.

The addition of a ducktail at the stern transom aims to make the water flow from the ship's hull to the rear more uniform. It also reduces the wetted transom effect, which causes waves and wakes to reduce wave-making resistance. A ducktail, basically Increasing the aft body length, is recommended for ferries with a Froude Number (Fr) of 0.2-0.3 or higher. It positively reduces ship resistance and can reduce power by about 4 – 7% [18]. Using ducktails also helps improve power efficiency on both new and existing ships. Following the installation element, the ducktail is one of the transom appendages besides the stern flap and stern wedge [16] and different geometrical alternatives [21].

So far, many studies have been carried out on ship hull AoE modifications and attachment of the ducktail, however, the research was carried out separately. Thus, the modification of AoE and ducktail in each specific case gives less than optimal to decrease the resistance of the ships.

The present research carried out is to combine the advantage of the modification of AoE and the addition of the ducktail. The research object of the 1,500 GT ro-ro ferry ship. Firstly, a numerical method was carried out to investigate/examine the magnitude of the reduction in resistance effect of the combination of modifications of AoE and ducktail. Secondly, the results are then verified by an experimental method by ship model resistance test in a towing tank.

Next, the results of the modification ones are analyzed through the uncertainty method to examine the validity of the CFD results and towing tests. Finally, the modification of both AoE and addition of ducktail are then compared with the original design prior to the modification one.

2.0 METHODOLOGY

This study uses numerical methods and experiments to determine the effect of hull shape modifications on the resistance value. Numerical simulations were carried out with the help of CFD-based computer programs by performing Numeca Fine Marine version 7.2. The experimental method was carried out by testing the ship model in the towing tank owned by the Hydrodynamic Technology Research Center-National Research and Innovation Agency (BRIN). The specifications of the Towing Tank used in the model test are as follows, length = 234.5 m (including port), width = 11.0 m, Water Depth = 5.5 m, Max. Acceleration = 1 m/s^2 and Max. Speed = 7 m/s. Due to its direct effect on the design process, valid and accurate resistance prediction results are obtained by validating and verifiying test results with numerical simulation results [22]. Numerical simulation and resistance testing were carried out under the same conditions with several variations of ship speed (Vs) from 10 knots to 18 knots with a draft of 3.30 meters.

2.1 Ship Data

As shown in Table 1 the object in this study is a 1,500 GT ro-ro ferry. The principal dimensions and other parameters of the "ship-model" are presented below.

Table 1 Principal dimensions, "Ship-Model" of 1,500 GT ro-ro ferry

Parameter	Notation	Original Design		Modification Design	
		Ship	Model	Ship	Model
Length Overall (m)	LOA	76.258	4.345	77.258	4.402
Length on waterline (m)	LWL	73.200	4.171	76.600	4.365
Breadth moulded on WL (m)	B	14.000	0.798	14.000	0.798
Depth moulded (m)	D	4.600	0.262	4.600	0.262
Draught moulded on FP (m)	TFP	3.300	0.188	3.300	0.188
Draught moulded on AP (m)	TAP	3.300	0.188	3.300	0.188
Displacement volume moulded (m3)	Δ	2196.620	-	2179.180	-
Mass density of water (ton,m3)	ρ	1.025	-	1.025	-
Wetted surface area bare hull (m2)	WSA	1223.991	3.974	1235.239	4.012
LCB position from AP (m)	LCB	32.660	1.861	32.443	1.849
Block coefficient	Cb	0.646		0.612	
Midship section coefficient	Cm	0.950		0.950	
Prismatic coefficient	Cp	0.680		0.645	
Angle of entrance (Degree)	iE	21		3	
Scale	λ	17.550			

2.2 Lines Plan

A body plan, Sheer plan, and half-breadth plan are included in the lines plan projection figure to show the overall shape of the hull [23]. Figure 1 is the lines plan (original design) with the AoE at the bow of the ship is 21 degrees, while Figure 2 shows the lines plan (modified design) by reducing the AoE at the bow from 21 degrees to 3 degrees at a draft condition of 3.30 meters (see detail B) and the addition of a ducktail to the stern transom (see detail A).

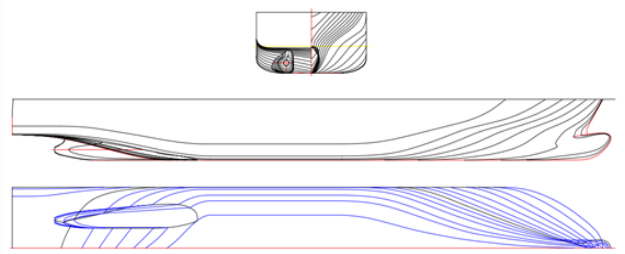

Figure 1 Lines plan ro-ro ferry (original design)

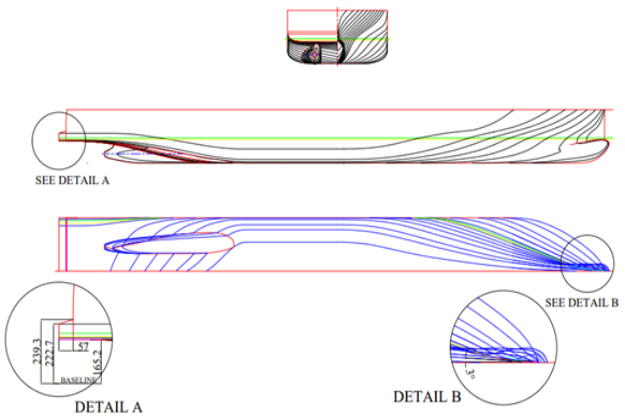

Figure 2 Lines plan ro-ro ferry (modification design)

2.3 Ship Model

After the model scale is determined, the next step is to determine the model ship dimension, displacement, and speed which are also converted to the same scale. The main material of the model is wood, produced in a ship model workshop (SMWS) equipped with several supporting types of equipment. The ship model was made using a laminated system with a fiberglass layer, with a ratio scale (λ) = 17.550.

2.4 Angle of Entrance

Drawings of half width on the lines plan can be used to determine half AoE (i_E), the amount of which is measured from the center line to the tangent line of the bow waterline at the specified draft [13, 24]. Reducing AoE causes wave resistance to decrease and the flow pattern from the front becomes better [12, 13, 20]. The wave resistance effect reduces as the AoE decreases, and vice versa. An explanation of AoE can be seen in Figure 3.

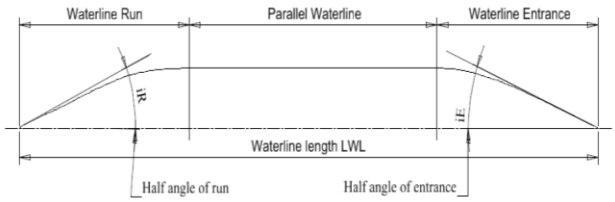

Figure 3 Angle of entrance

2.5 Ducktail

The correlation of the shape of the transom with the flow field and resistance is the reason for making the optimal stern design [25]. Ducktail is a device that helps to reduce the wetted transom effect, which causes waves and wakes [18]. Based on Froude's numbers, the ducktail can significantly reduce the ship's resistance. The ducktail is one of the schemes in the stern transom [16], basically an extension of the stern [17]. Figure 4 shows the addition of a ducktail on the stern transom of a ship.

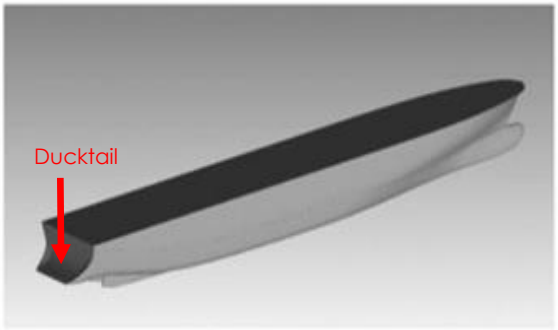

Figure 4 Ducktail on the stern transom

2.6 Ship Resistance

In general, the ship's total resistance can be broken down into several basic components: frictional resistance (Rf), pressure resistance (Rp), wave resistance (Rw), and air resistance (Ra) [26] and [27]. The international standard ITTC-1957 also divides ship resistance in calm waters into two components: viscous resistance related to Reynolds number (Rn) and wave resistance related to Froude number (Fn). The equation for determining the resistance of the full-scale model is as follows:

$$R_T = \frac{1}{2}.\rho.Vs^2.WSA.C_T \quad (1)$$

In the formula for total resistance (R_T) in Newton (N), where ρ is the water density (kg/m^3), Vs is the ship's speed (m/s), WSA is the Wetted Surface Area (m^2), and C_T is the ship's total resistance coefficient.

2.7 Numerical Method

The numerical method uses numbers, algorithms, and computer assistance to solve mathematical formulas for fluid flow patterns. The basis for calculating CFD is the Navier-Stokes equation which shows the relationship between the conservation of momentum, mass, and energy in fluids. The problem limitation in this numerical method is that the surface roughness value of CFD numerical simulation modeling is ignored, which is useful for the effectivity of calculations. Numerical methods are used to analyze the resistance and the components affecting it [28] to estimate the ship's total resistance value before the resistance test is performed. Prediction of ship resistance from numerical simulation (CFD) must be able to support the towing tank test [29].

Data retrieval is carried out by processing the principal dimensions and lines plan, then based on CFD analysis using computer software, the resistance values, and fluid flow characteristics along the ship's hull are obtained. Modeling is done by converting the lines plan image into a 3D surface shape and then making it a solid model in Parasolid format (x.t). Figure 5 shows the original design of hull modeling, while Figure 6 presents the modified design of hull modeling at the bow AoE (see B) and the addition of a ducktail at the stern transom (see A).

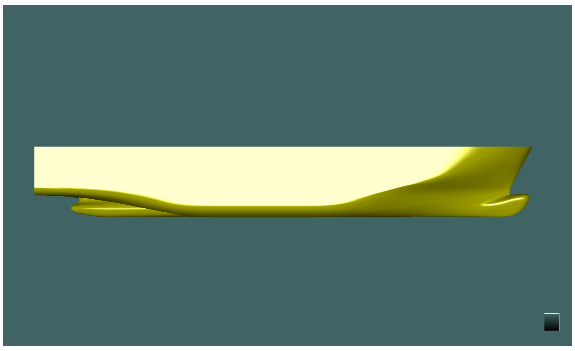

Figure 5 Hull modeling (original design)

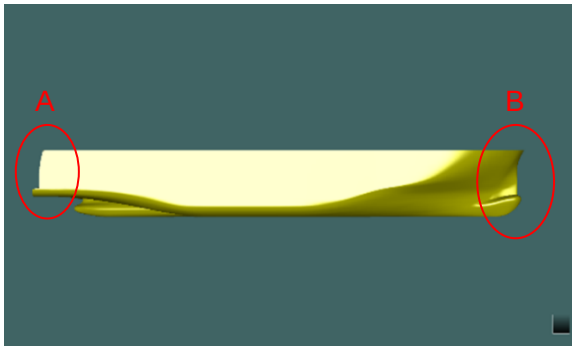

Figure 6 Hull modeling (modification design)

At the simulation stage, there are 3 (three) steps: domain creation, meshing model, and parameter setting. The resistance numerical simulation is made using a half-body domain, so the final results must be multiplied by 2. Based on several studies related to CFD simulations, the domain size has quite a variety of variations, according to [30, 31, 32]. This study determined the size and process of creating domains used in numerical simulations, as shown in Figures 7 and Figure 8.

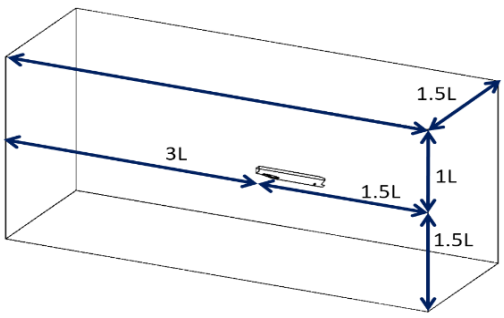

Figure 7 Domain size

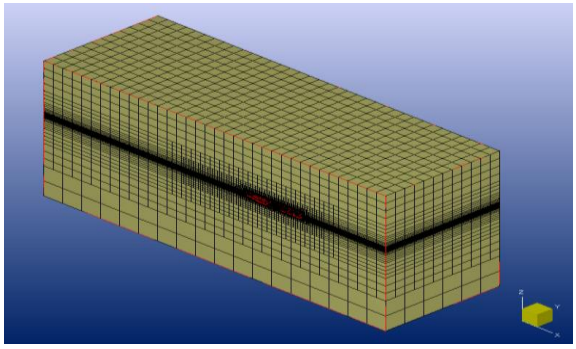

Figure 8 Meshing model

In the next process, meshing is carried out through 5 (five) steps, namely, Initial mesh, Adapt to Geometry, Snap to Geometry, Optimize, and Viscous Layers. Furthermore, at the parameter setting stage, the settings are adjusted to the ship's condition when conducting experiments in the towing tank. It is related to the waterline depth, ship speed, and simulation iteration settings. Data validation is important in numerical simulation to ensure the results are correct and accurate. 2 (two) things can be used as a reference: convergent and grid-independent. Convergence is the value of the simulation iteration process that must reach the smallest error value, where the convergence line is shown in Figure 9. below. While the independent grid is the optimum position value from several simulations where the difference in the calculation value of the number of elements with the last element is less than 5% [33], grid independence is presented in Figure 10.

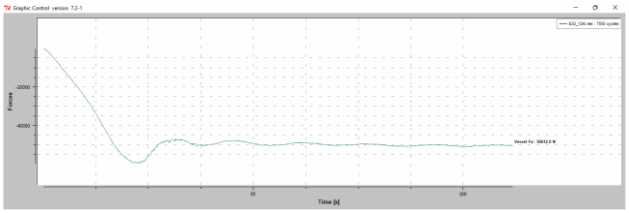

Figure 9 Convergent lines

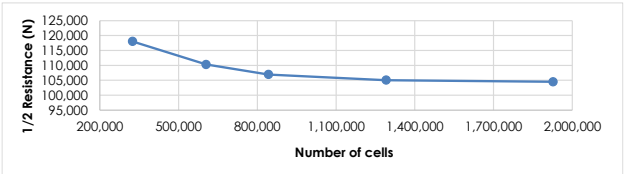

Figure 10 Independence grids

Table 2 Effect of number of elements on resistance value

Meshing	Resistance (N)	Gaps
324,912	118,024	N/A
605,103	110,290	-7.01%
842,807	106,913	-3.16%
1,290,922	105,052	-1.77%
1,927,242	104,468	-0.56%

From the simulations carried out to obtain grid independence, it is found that the number of cells/grid of 842,807 has met the specified criteria or limits, see Table 2.

The advantages of CFD compared to experimental methods are as follows: CFD simulation can be run in a short time, costs are relatively low, and it provides the ability to theoretically simulate any physical conditions (real conditions) with results that are close to the truth [34].

2.8 Uncertainty of Analysis in CFD

The uncertainty analysis of results generated through Reynolds-averaged Navier Stokes (RANS) equations was performed according to the recommendations of ITTC [35, 36]. Grid studies were conducted using four grids and estimating grid errors and uncertainties using three grids (e.g., grids1-3 and grids 2-4). Convergence studies of three solutions were conducted to evaluate the convergence concerning the input parameter. Changes in the three solutions were used to define.

$$R_G = \varepsilon_{G,21} / \varepsilon_{G,32} \tag{2}$$

Where R_G is the convergence ratio, $\varepsilon_{G,21}$ is a fine-medium error, and $\varepsilon_{G,32}$ is a medium-coarse error. Richardson extrapolation (RE)-based methods i-th the three solutions were used to provide one-term estimates for error and order of accuracy:

$$\delta^*_{RE_G} = \frac{\varepsilon_{G,21}}{r_G^{P_G} - 1} \tag{3}$$

$$P_G = \frac{l(\varepsilon_{G,32} / \varepsilon_{G,21})}{\ln(r_G)} \tag{4}$$

An factor of safety (FS) approach [37] was used to determine the grid uncertainty of the finest mesh, wherein an error estimate from RE was multiplied by an FS to bound simulation errors.

$$U_G = (F_s - 1)\left|\delta^*_{RE_G}\right| \tag{5}$$

Validation was applied to assess simulation modeling uncertainty U using the experimental data-adopted V&V 20 2009 Standard [38]. Therefore, the numerical uncertainty U_{SN} was equal to the grid uncertainty U_G [39]. The validation uncertainty is calculated as:

$$U_V^2 = U_D^2 + U_G^2 \tag{6}$$

Where U_D is the uncertainty of model test.

2.9 Experimental Method

The physical model test must be extrapolated and meet the requirements of the law of similarity from the model to the full-scale ship [40]. All devices used

in the model test for data acquisition should be calibrated regularly. The measured quantities should be substituted with calibrated scales and pulses or checked with other calibrated measuring devices for calibration. Furthermore, the ship model is connected to the Towing point, which is installed in line with the centerline of the towing tank and at the center of the flotation position of the ship model to the force measuring device, namely the resistance dynamometer. The resistance force is recorded by a measuring instrument that shows the required resistance and is related to determining the ship's thrust to reach a certain speed.

Basically, all resistance testing in towing tanks follows the rules of the ITTC. One of the ITTC requirements in ship testing is carried out in calm water conditions (ideal trial conditions), meaning there is no wind, current, or waves. Furthermore, accommodating and overcoming natural phenomena such as the above related to shipping operations usually added a sea power margin of 15% of the results of self-propulsion testing. So the running software that is carried out must follow the conditions of the actual ship model test on the towing tank.

2.10 Uncertainty Analysis for Resistance

Experimental process uncertainty assessment as recommended by the International Towing Tank Conference (ITTC) [41, 42]. The equations used to estimate the relative standard uncertainty component of the resistance related to the hull geometry are:

$$u_1^{'}(R_T) = u^{'}(S) = \frac{2}{3}u^{'}(\Delta) \quad (7)$$

Where u'(S) is the uncertainty component of the wetted surface area, Δ is the uncertainty component of the displacement volume of the ship model. While the resistance uncertainty due to towing speed is:

$$u_2^{'}(R_T) = 2u^{'}(V) \quad (8)$$

Where *u'(V)* is the uncertainty of the towing speed. The relative standard uncertainty of resistance is estimated with equation:

$$u_3^{'}(R_T) = \frac{C_F}{C_T}\frac{0.87}{\log_{10}\mathrm{Re} - 2}u^{'}(v) \quad (9)$$

Where C_F is the coefficient friction, C_T is the total resistance coefficient, Re is the Reynold's number, and *u'(v)* is the uncertainty component of the water viscosity affected by temperature. The uncertainty component of the resistance resulted from the calibration of the dynamometer is estimated by standard error estimation (SEE).

$$u_4^{'}(R_T) = SEE \quad (10)$$

The standard uncertainty component from single test tests can be estimated with the following equation:

$$u_5^{'}(R_T) = s \quad (11)$$

Then combined to obtain the overall standard uncertainty by the rootsum-squares method.

$$u_c^{'} = \sqrt{(u_1^{'})^2 + (u_2^{'})^2 + (u_3^{'})^2 + (u_4^{'})^2 + (u_5^{'})^2} \quad (12)$$

The expanded standard uncertainty of the resistance with confidence level (t table) is estimated using Equation:

$$u_P(R_T) = k_{p.}u_c^{'}(R_T) \quad (13)$$

Where k_p is the coverage factor.

2.11 Determination of the Ship's Resistance

The steps for calculating resistance by extrapolation from the model to the full-scale ship (ITTC-1957) are as follows:

- According to Froude, the coefficient of total ship resistance (C_T) will be obtained from the ship model test.

$$C_{T(\mathrm{mod}\,el)} = C_{F(\mathrm{mod}\,el)} + C_{R(\mathrm{mod}\,el)} \quad (14)$$

$$C_{T(\mathrm{mod}\,el)} = \frac{R_{T(\mathrm{mod}\,el)}}{1/2.\rho.WSA_{(\mathrm{mod}\,el)}.V^2_{(\mathrm{mod}\,el)}} \quad (15)$$

- While the coefficient of frictional resistance (C_F) is obtained from the calculation with the equation:

$$C_F = \frac{0.075}{(\log_{10} R_n - 2)^2} \quad (16)$$

- Prediction of form factors (1+k) [43, 44], obtained using the Prohaska method [45, 46].
- The coefficient of total vessel resistance (C_T) and Correlation Allowance (C_A) [24] is the additional coefficient to the ship model's correlation resistance. The ITTC-1957 coefficient of friction resistance formula must be combined between model - ship with Form Factor (1+k) [43], namely:

$$C_{T(ship)} = C_{T(\mathrm{mod}\,el)} - (1+k)(C_{F(ship)} - C_{F(\mathrm{mod}\,el)} + C_A) \quad (17)$$

$$C_A = 0.006(L+100)^{-0.16} - 0.00205 \quad (18)$$

- So that the total value of the ship's total resistance (R_T) can be obtained.

3.0 RESULTS AND DISCUSSION

The results of numerical simulations and model tests of the modified design are then analyzed, validated and compared.

3.1. Numerical Simulation Results

Calculations Numerical simulation of the 1,500 GT ro-ro ferry was carried out at draft conditions (T) = 3.30

m with several variations of ship speed (Vs) ranging from 10 knots to 18 knots. Because the resistance value obtained from the CFD numerical simulation calculation is the resistance value of half the hull, this value must first be multiplied by 2 to obtain the appropriate total resistance value of the entire hull.

Figure 11 is the result obtained from the numerical simulation of the original design at a speed (Vs) of 16 knots. Visually, it can be seen that the appearance of the circulation zone can cause a wetted transom effect which has a negative impact on increasing resistance, causing waves, breaking of waves, and spray behind the transom, which is not fully transmitted to the far field. Since the wake cannot be transmitted far away from the aft body, eddy currents cannot be generated to absorb energy. High vortex concentration can increase the pressure causing a decrease in speed. Meanwhile, Figure 12 shows the modified design numerical simulation results. The addition of a ducktail at the stern causes the circulation zone to decrease so that the flow of water forward to the aft ship becomes uniform, and the wetted transom effect, which causes waves and wakes to form at the stern, is reduced. So that causes the pressure to decrease, and the speed can increase for the better. The effect of bow AoE modifications can be explained in Figure 15 and Figure 16 below.

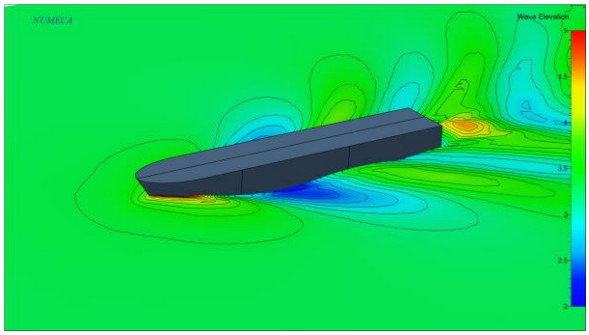

Figure 11 Numerical simulation results (original design) at Vs = 16 knots

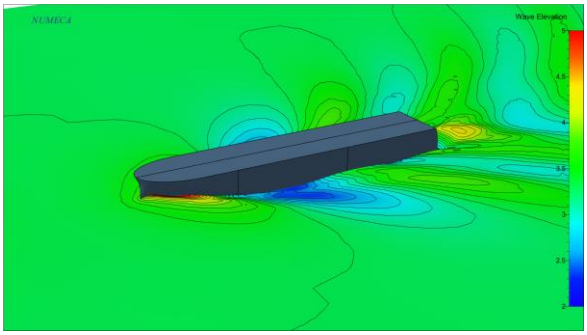

Figure 12 Numerical simulation results (modification design) at Vs = 16 knots

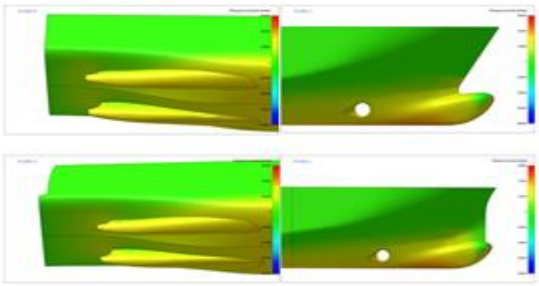

Figure 13 Pressure distribution on front and stern hull form of ro-ro 1,500 GT

Visualization of the pressure contour at 16 knots can be observed in Figure 13. The color legend scale is ranging from -8000 N/m2 until 6000 N/m2. The water flow from the bow is turned following hullshape, some area coloured with dark red marking that the pressure is still high in that area. The high local pressure because the bulb and ducktail obstruct the water flow.

Table 3 shows the difference in total ship resistance values obtained from CFD numerical simulation results on the original and modified designs.

Table 3 CFD numerical simulation results of original and modification design

Speed (Vs)	Numerical simulation (CFD)			
	Original Design		Modification Design	
(Knots)	1/2 R_T (N)	R_T (N)	1/2 R_T (N)	R_T (N)
10	33,940	67,880	29,932	59,864
11	40,758	81,516	37,318	74,636
12	50,396	100,792	44,136	88,272
13	61,225	122,450	53,185	106,370
14	79,238	158,476	67,057	134,114
15	112,907	225,814	88,583	177,166
16	135,920	271,840	113,236	226,472
17	157,451	314,902	133,735	267,470
18	176,668	353,336	152,800	305,600

Meanwhile, Figure 14 illustrates the shape of the ship's resistance curve, which shows the relationship between the total resistance at each speed obtained from the numerical simulation of the original and modified designs.

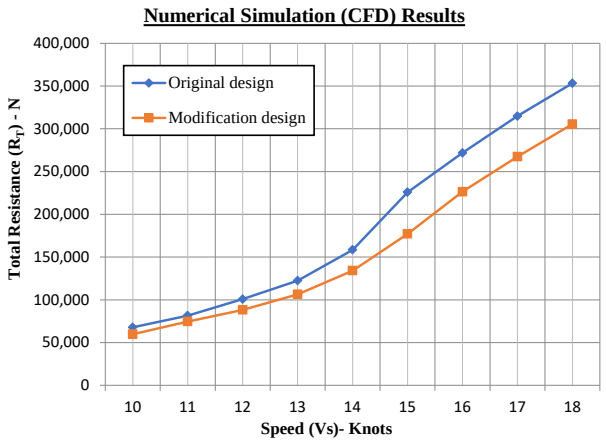

Figure 14 Resistance (R_T) - Speed (Vs) curve
Numerical simulation (CFD) results from the original design - modification design

3.2. Ship Model Resistance Test

The ship model resistance test was performed under the same conditions and speeds as the numerical simulation. The total resistance value results of the model test must be extrapolated from the model to the ship at full scale. In the resistance test, in addition to the total resistance value (R_T), the Effective Horse Power (EHP) value is also obtained.

AoE modifications have a significant effect on the flow patterns that occur at the fore of the ship. In testing the resistance of the ship model in the towing tank with a ship speed (Vs) of 16 knots, visually it can be seen that the flow in the initial design model occurs with a very large spray towards the top and sides, see Figure 15. This is different from the modified design model, where at a speed the same spray occurs smaller, lower near the surface of the water, as shown in Figure 16. And the phenomenon of spray or waves generated by the hull will increase at higher speeds. This condition is minimized in the modified design.

Figure 15 Ship model resistance test (original design)

Figure 16 Ship model resistance test (modification design)

Table 4 below presents the total resistance value results of the ship model resistance test in the towing tank.

Table 4 Ship model resistance test results of original and modification design

Speed (Vs)	Ship model resistance test	
	Original Design	Modification Design
(Knots)	R_T (N)	R_T (N)
10	64,500	57,000
11	79,900	71,000
12	99,500	86,000
13	125,000	105,000
14	163,000	135,000
15	216,000	178,000
16	272,000	227,000
17	323,000	270,000
18	371,000	310,000

Meanwhile, in Figure 17 shows the total resistance curve of the ship model resistance test results on the towing tank in the original and modified designs.

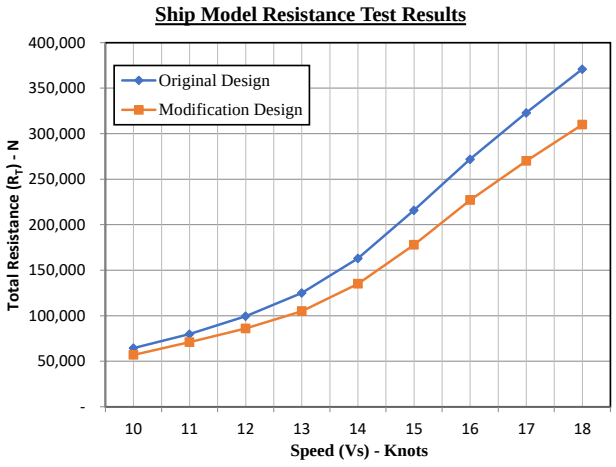

Figure 17 Resistance (R_T) - Speed (Vs) curve
Experiment results from the original design - modification design

Figure 18 below shows a comparison of the shape of the total resistance curve of the original and the modified designs obtained from the numerical simulation and the ship model resistance test. From the data in the table and curves below, it can be seen that the total resistance value from the numerical simulation and the ship model resistance test in the original design shows a value that is relatively close to or almost the same. Compared with the ship model resistance test, the numerical simulation results on the modified design show a lower value.

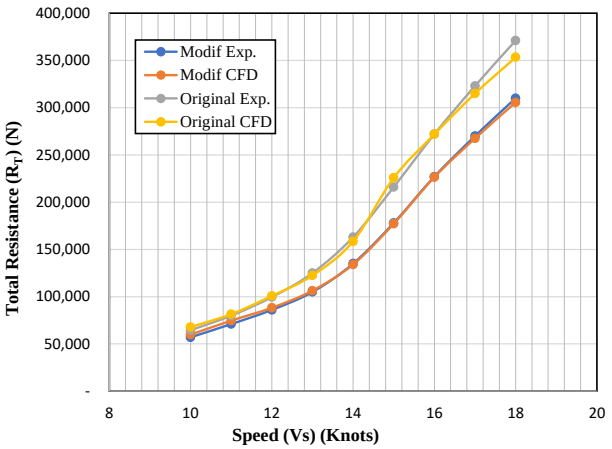

Figure 18 Resistance (R_T) - Speed (Vs) curve Numerical simulation (CFD) and experiment results from the original design - modification design

The resistance curve graph above shows the same pattern of increasing ship resistance between the results of numerical simulations and ship model resistance test and begins to experience differences in increase after a speed of 14 knots. The results of both methods show good agreement, and the difference between them increases with increasing ship speed. In this case, the reduction in wave resistance due to the modification of the hull form at the AoE and the addition of the ducktail at the stern transom greatly influences in reduction of total ship resistance. Other resistance components, namely frictional resistance related to Wetted Surface Area and pressure resistance due to the shape of the hull underwater, have little effect because they do not change much.

3.3. Uncertainty Analysis Results

V&V results are presented in Table 5. The convergence condition corresponds to three solutions, as the monotonic convergence was achieved with R of <1. Every three grids adopted the same refinement ratio r_G = √2. The validation uncertainty for the finest grid for all *Fr* values was <4%.

Table 5 V & V result

R_G	P_G	U_G	U_D	U_{val}
0.37	2.69	0.36%	0.55%	0.77%
0.68	1.07	0.59%	0.51%	0.73%
0.36	2.84	0.34%	0.49%	0.66%

The predominant sources of uncertainty in the resistance measurements were investigated using the ITTC method. The standard uncertainty of resistance consists of several components, i.e. hull ballasting, instrument calibration, water temperature, towing speed and direct measurement. It can be seen that the measurement uncertainty in the resistance tests for this hull model was estimated at about 0.016% to 1.109% at speed (Vs) 13 knots, about 0.007% to 1.003% at speed (Vs) 16 knots and 0.005% to 0.989% at speed (Vs) 18 knots, , are summarized in Table 6. Coverage kp = 2 corresponds to a confidence level of 95% for a single test.

Tabel 6 Analysis of uncertainty for resistance measurement (water temperature 27.3°C)

Uncertainty component	Speed (knots) 13	16	18
Hull balasting	0.458%	0.212%	0.155%
Towing speed	0.067%	0.067%	0.067%
Water temperature	0.031%	0.017%	0.016%
Dynamometer	0.016%	0.007%	0.005%
Single test, deviation	0.252%	0.054%	0.029%
Combined for single	0.528%	0.221%	0.159%
Expanded for single	1.109%	1.003%	0.989%

4.0 CONCLUSION

Based on the results and discussion of the entire numerical simulation process and ship model resistance test, it can be concluded that the reduction in total resistance at speeds of 13 - 18 knots due to the influence of AoE modifications ranged from 8.89% - 12.19% and ducktails between 3.12% - 3.62%. While the combination of AoE and the addition of the ducktail from the results of numerical simulation (CFD) and ship model resistance test in towing tanks at the same speed shows that the total resistance of the ship is reduced between 13.13% - 16.69% and 16.00% - 16.54 %.

The results of the numerical simulation (CFD) and ship model resistance test show an average difference of 0.325% and 0.188% at each speed for the original design and the modified design, respectively.

AoE modification can improve the flow pattern and reduce the spray at the ship's bow. Meanwhile,

the emergence of a circulation zone due to the addition of ducktails can be minimized so that waves and wakes at the stern of the ship decrease. These findings show that Design modifications by decreasing the bow AoE and adding a ducktail retrofit on the stern transom significantly reduce the total resistance of the ship. The numerical simulation results used to an initial overview to predict ship resistance's value before the model test.

Conflicts of Interest

The author(s) declare(s) that there is no conflict of interest regarding the publication of this paper.

Acknowledgment

The authors would like to thank the National Research and Innovation Agency (BRIN) for funding the research under the Degree by Research 2021 scheme with contract number: SP/114/BPPT/08/2021. I would like to express my appreciation to my supervisor and all those who supported this research.

References

[1] Al Syahrin, M., N. 2018. Jokowi's Maritime Axis Policy and the Synergy of Indonesia's Maritime Security and Economic Strategy (In bahasa Indonesia). *Indonesian Perspective*. 3(1): 1-17. Doi: https://dx.doi.org/10.14710/ip.v0i0.20175.

[2] Elkafas, A. G., Khalil, M., Shouman, M. R., & Elgohary, M. M. 2021. Environmental Protection and Energy Efficiency Improvement by using Natural Gas Fuel in Maritime Transportation. *Environmental Science and Pollution Research*. 28(43): 60585-60596. Doi: https://doi.org/10.1007/s11356-021-14859-6.

[3] Utama, I. K. A. P. 2018. Potential for Improvement of Future Ship Efficiency: Overview of Ship Design and Operational Aspects (In bahasa Indonesia). *ALE Proceeding*. 1(April): 1-15. DOI: https://dx.doi.org/10.30598/ale.1.2018.1-15.

[4] Tokuşlu, A. 2020. Analyzing the Energy Efficiency Design Index (EEDI) Performance of a Container Ship, Chief in Editor. *International Journal of Environment and Geoinformatics (IJEGEO)*. 7(2 August): 114-119. DOI: https://dx.doi.org/10.30897/ijegeo.703255.

[5] Barreiro, J., Zaragoza, S., Diaz-Casas, V. 2022. Review of Ship Energy Efficiency. *Ocean Engineering*. 257(January): 111594. Doi: https://dx.doi.org/10.1016/j.oceaneng.2022.111594.

[6] Zhao, C., Wang, W., Jia, P., Xie, Y. 2021. Optimisation of Hull Form of Ocean-going Trawler. *Brodogradnja*. 72(4): 33-46. Doi: https://dx.doi.org/10.21278/brod72403.

[7] Susilo, J., Santoso, A., & Musyiradi, T. B. 2013. Simulation of the Use of Fin Undership on Resistance and Ship Thrust with the CFD Analysis Method (In bahasa Indonesia). *Jurnal Teknik Pomits*. 3(2): 2337-3539.

[8] Afrizal, E., & Koto, J. 2018. Effect of Bulbous Bow on Ice Resistance of Ice Ship. *Journal of Ocean, Mechanical and Aerospace*. 60(1): 7-17.

[9] Baiju, M. V, Vipinkumar, V., Dhijudas, P. H., Sivaprasad, K., & Edwin, L. 2022. A Study on the Influence of Bulbous bow on the Resistance of Fishing Vessel Hull form Using CFD Analysis. June.

[10] Malek, M. A. bin A., & J.Koto. (2017). Study on Resistance of Stepped Hull Fitted With Interceptor. Journal of Ocean, Mechanical and Aerospace, Science and Engineering, 39(39), 18–22.

[11] Setiabudi, Z. T., Utama, I. K. 2020. CFD Analysis of Catamaran Barriers with Transverse Stepped Hull (In bahasa Indonesia). *Jurnal Teknik ITS*. 9(2): 1-8. Doi: https://dx.doi.org/10.12962/j23373539.v9i2.56581.

[12] Ivandri, H., Mulyatno, I. P., Kiryanto. 2017. The Influence of Entry Angle on 750 Dwt Pioneer Ships on Ship Resistance With the Addition of Anti-Slamming Bulbous Bow Delta Type (Δ – Type) (In bahasa Indonesia). *J. Tek. Perkapalan*. 5(4): 785. Doi: https://dx.doi.org/10.1051/matecconf/201815901057.

[13] Hadi, E. S., Manik, P., & Iqbal, M. 2018. Influence of Hull Entrance Angle Perintis 750 DWT, Toward Ship Resistance: The Case Study For Design Development Perintis 750 DWT. *MATEC Web of Conferences*. 159: 2-7.

[14] Cahyadi Sugeng, J. M., Semin, & Erwandi. 2022. The Study of the Modification of the Ro-Ro Ferry's Angle of the Entrance using Statistical Methods and Ship Model Resistance Tests. *IOP Conference Series: Earth and Environmental Science*. 1081(1). Doi: https://dx.doi.org/10.1088/1755-1315/1081/1/012018.

[15] Samuel, S., Timoty Frans Evan S., S., Trimulyono, A., & Iqbal, M. 2022. An Analysis of the Effect of the Bow Entrance Angle on Ship Resistance. *Sinergi*. 26(2): 223. DOI: https://dx.doi.org/10.22441/sinergi.2022.2.011.

[16] Jang, H. S., Lee, H. J., Joo, Y. R., Kim, J. J., Chun, H. H. 2009. Some Practical Design Aspects of Appendages for Passenger Vessels. *International Journal of Naval Architecture and Ocean Engineering*. 1(1): 50-56. Doi: https://dx.doi.org/10.2478/IJNAOE-2013-0006.

[17] Richards, J. S., Reinholz, O. 2011. Hydrodynamic Trends in Ferry Design. *11th International Conference on Fast Sea Transportation, FAST 2011 - Proceedings*, September, 382-386. http://resolver.tudelft.nl/uuid:bc9550e9-f215-44a3-bceb-258dcccfb850

[18] Kurniawati, F. D., Pria Utama, I. K. A. 2017. An Investigation into the Use of Ducktail at Transom Stern to Reduce Total Ship Resistance. *IPTEK Journal of Proceedings Series*. 0(2): 181. DOI: https://dx.doi.org/10.12962/j23546026.y2017i2.2338.

[19] Cho, Y., Hwangbo, S. M., Yu, J.-W., Lee, J., Park, Y., Jang, W.-H., & Lee, I. 2023. Improvement of Hull Form for an 1,800 TEU Containership Toward Reduced Fuel Consumption Under In-service Conditions. *International Journal of Naval Architecture and Ocean Engineering*. 15: 100520. Doi: https://dx.doi.org/10.1016/j.ijnaoe.2023.100520.

[20] Kristensen, H. O., & Lützen, M. 2013. Prediction of Resistance and Propulsion Power of Ships. Project No. 2010-56, Emissionsbeslutningsstøttesystem. 4(2010): 52. http://www.skibsteknisk selskab.dk/public/dokumenter/Skibsteknisk/Foraar 2013/25.02.2013/WP 2 - Report 4 - Resistance and Propulsion Power - FINAL - October 2012.pdf.

[21] Silva-Campillo, A., Suárez-Bermejo, J. C., & Herreros-Sierra, M. A. 2022. Design Recommendations for Container Ship Side-shell Structure under Fatigue Strength Assessment. *Ocean Engineering*. 246. DOI: https://dx.doi.org/10.1016/j.oceaneng.2022.110655.

[22] Xhaferaj, B., 2022. Investigation on Some Conventional Hulls Forms of the Predictive Accuracy of a Parametric Software for Preliminary Predictions of Resistance and Power. *Brodogradnja*. 73(1): 1-22. Doi: https://dx.doi.org/10.21278/brod73101.

[23] Wilson, P. A. 2018. Basic Naval Architecture: Ship Stability. *Basic Naval Architecture: Ship Stability*. 1-203. Doi: https://dx.doi.org/10.1007/978-3-319-72805-6.

[24] Lewis, E. V. 1988. Principles of Naval Architecture, Second Revision. Volume 2: Resistance, Propulsion and Vibration Chapter 5 Manen, JD v, Resistance, Chapter 6 Manen, JD v, Propulsion, Chapter 7 Vorus, WS, Vibration. EV Lewis,

Editor. The Society of Naval Architects and Marine Engineers, SNAME, Jersey City, New York, USA.
[25] Duy, T.-N., Hino, T., Suzuki, K. 2017. Numerical Study on Stern Flow Fields of Ship Hulls with Different Transom Configurations. *Ocean Engineering*. 129: 401-414. Doi: https://dx.doi.org/10.1016/j.oceaneng.2016.10.052.
[26] Dinham-Peren, T. 2010. Marine Propellers and Propulsion, 2nd edition. *Proceedings of the Institution of Civil Engineers - Maritime Engineering*. 163(4). Doi: https://dx.doi.org/10.1680/maen.2010.163.4.182.
[27] Molland, A. F., Turnock, S. R., Hudson, D. A. 2011. Ship Resistance and Propulsion: Practical Estimation of Ship Propulsive Power. *Ship Resistance and Propulsion: Practical Estimation of Ship Propulsive Power*. 9780521760. Doi: https://dx.doi.org/10.1017/CBO9780511974113.
[28] Terziev, M., Tezdogan, T., Incecik, A. 2022. Scale Effects and Full-scale Ship Hydrodynamics: A Review. *Ocean Engineering*. 245(January): 110496. Doi: https://dx.doi.org/10.1016/j.oceaneng.2021.110496.
[29] Niklas, K., Pruszko, H. 2019. Full-scale CFD Simulations for the Determination of Ship Resistance as a Rational, Alternative Method to Towing Tank Experiments. *Ocean Engineering*. 190(April): 106435. Doi: https://dx.doi.org/10.1016/j.oceaneng.2019.106435.
[30] Purnamasari, D., Utama, I. K. A. P., Suastika, I. K. 2018. CFD Simulations to Calculate the Resistance of A 17.500-DWT Tanker. *IPTEK Journal of Proceedings Series*. 4(1): 112. DOI: https://dx.doi.org/10.12962/j23546026.y2018i1.3519.
[31] Chiroșcă, A. M., Rusu, L. 2021. Comparison between Model Test and Three CFD Studies for a Benchmark Container Ship. *Journal of Marine Science and Engineering*. 9(1): 1-16. Doi: https://dx.doi.org/10.3390/jmse9010062.
[32] Prihandanu, R. B., Ariana, I. M., Handani, D. W. 2021. Analysis of Stern Shape Effect on Pre-Duct Propeller Performance Based on Numerical Simulation. *IOP Conference Series: Materials Science and Engineering*. 1052(1): 012016. Doi: https://dx.doi.org/10.1088/1757-899X/1052/1/012016.
[33] Molland, A. F., Utama, I. 2002. Experimental and Numerical Investigations into the Drag Characteristics of a Pair of Ellipsoids in Close Proximity. *Proceedings of the Institution of Mechanical Engineers, Part M: Journal of Engineering for the Maritime Environment*. 216(2): 107-115. Doi: https://dx.doi.org/10.1243/147509002762224324.
[34] Vu, N. K., & Nguyen, H. Q. 2020. Numerical Simulation of Flow around the Ship using CFD Method. *Journal of Mechanical Engineering Research and Developments*. 43(7): 75-86.
[35] ITTC. 2017. Uncertainty Analysis in CFD Verification and Validation Methodology and Procedures. ITTC - Recommended Procedures and Guidelines. 1-13.
[36] Utama, I. K. A. P., Purnamasari, D., Suastika, I. K., Nurhadi, & Thomas, G. A. 2021. Toward Improvement of Resistance Testing Reliability. *Journal of Engineering and Technological Sciences*. 53(2). Doi: https://dx.doi.org/10.5614/j.eng.technol.sci.2021.53.2.1.
[37] Roache, P. J. 1998. Verification of Codes and Calculations. *AIAA Journal*. 36(5): 696-702. Doi: https://dx.doi.org/10.2514/2.457.
[38] ASME V&V, 20. 2009. Guide on Verification and Validation in Computational Fluid Dynamics and Heat Transfer.
[39] Stern, F., Wilson, R. V, Coleman, H. W., & Paterson, E. G. 2001. Comprehensive Approach to Verification and Validation of CFD Simulations - Part 1: Methodology and Procedures. *Journal of Fluids Engineering*. 123: 793-802.
[40] ITTC. 2002. Guidelines: Testing and Extrapolation Methods: Resistance-Uncertainty Analysis, Example for Resistance Test. ITTC Recommended Procedures and Guidelines, Procedure. 5-7.
[41] ITTC. 2014. General Guideline for Uncertainty Analysis in Resistance Tests - Procedure 7.5-02 -02-02. Recommended Procedures. 1-10.
[42] Purnamasari, D., Utama, I. K. A. P., & Suastika, I. K. 2020. Verification and Validation of a Resistance Model for Tanker 17.500 dwt. *Journal of Marine Science and Technology (Taiwan)*. 28(1): 18-24. Doi: https://dx.doi.org/10.6119/JMST.202002_28(1).0003.
[43] Hughes, G. 1954. Friction and Form Resistance in Turbulent Flow, and a Proposed Formulation for Use in Model and Ship Correlation. National Physical Laboratory, NPL, Ship Division, Presented at the Institution of Naval Architects, Paper No. 7, London, April, RINA Transactions. 1954-16.
[44] Korkmaz, K. B., *et al*. 2021. CFD based Form Factor Determination Method. *Ocean Engineering*. 220(September 2020): 108451. Doi: https://dx.doi.org/10.1016/j.oceaneng.2020.108451.
[45] Prohaska, C. W. 1966. A Simple Method for the Evaluation of the Form Factor and the Low Speed Wave Resistance. Hydro-and Aerodynamics Laboratory, Lyngby, Denmark, Hydrodynamics Section. *Proceedings of the 11th International Towing Tank Conference, ITTC'66*, Tokyo, Japan, Resistance Committee. 65-66.
[46] Widodo, Santoso, A., Erwandi, Baidowi, A. 2022. Form Factor Prediction based on Ship Model Test Data by Statistical Method. *IOP Conference Series: Earth and Environmental Science (Mastic)*. 1081: 0-12. Doi: https://dx.doi.org/10.1088/1755-1315/1081/1/012017.